JOURNAL OF MATERIALS SCIENCE 20 (1985) 2186–2192

Forming, negative resistance, pressure effect, dielectric breakdown and electrode diffusion in thin SiO_x films with laterally spaced electrodes

S. A. Y. AL-ISMAIL, C. A. HOGARTH
Department of Physics, Brunel University, Uxbridge, Middlesex, UK

The sample structure consists of two laterally spaced copper electrodes joined by a thin silicon monoxide film (type B). The forming effect in type B samples is compared with the forming effect in the conventional MIM sandwich structure (type A). In type A devices two extreme cases of forming are shown; one is the typical forming effect and the other is an initial highly conductive state, leading to a reduction in current and to a more normal electro-formed characteristic after a sudden change in current at a fairly high applied voltage. The important point in the two cases is that the ultimate formed characteristic is the same for both cases and is independent of the initial *V–I* characteristic. Type B samples exhibit the highly conductive state characteristic of type A samples after breakdown occurs. This breakdown behaviour is believed to be associated with the power lost in the sample. Similar voltage-controlled negative resistance (VCNR) is observed in type B samples to that of type A samples. The development of this VCNR and the effect of ambient pressure on this characteristic is explained. Microprobe analysis study of type B samples shows the diffusion of metal in the insulator, which may account for the electro-forming effect.

1. Introduction

Since the work of Kreynina *et al.* [1] a considerable interest has been shown in thin film sandwich structures which exhibit forming effects. Oxides have been extensively studied, particularly SiO_x [2–8]. Prior to forming, in the conventional MIM sandwich structures, a $\log I_c \propto V_b^{1/2}$ dependence is frequently shown [9], where I_c is the circulating current through the device and V_b is the applied voltage. Such plots are normally taken to be an indication of the Schottky or Poole–Frenkel effect, and although there is considerable controversy regarding the interpretation of such curves [4, 10], these conduction mechanisms have no influence on the after-forming characteristics, and will therefore be disregarded in the following discussion. However, we should mention that a discontinuous gold film on an insulating substrate in a planar arrangement gave characteristics attributed to Schottky emission as the main high-field transport mechanism but with space-charge effects and tunnelling from island to island taking place [11]. For SiO_x films between laterally spaced electrodes in a planar arrangement, a $\log I_c \propto V_b^{1/4}$ dependence is shown, which is explained in terms of Schottky emission due to a blocking contact as the dominant process, with some contribution from hopping conduction, particularly at low temperature [8].

Forming is initiated by the application of a voltage in excess of the forming voltage V_F. For SiO_x, values of V_F as low as 1.9 V have been reported [7]. During forming the current increases to a level higher than that before forming. After forming the samples usually display a differential negative resistance, electron emission, memory effects and electroluminescence. A review of these effects is given by Dearnaley *et al.* [12]. Several

0022–2461/85 $03.00 + .12

models explaining the operation of such samples have been proposed in terms of isoenergetic tunnelling [2, 9, 13], solid state electrolysis [14] and a combination of ionic and tunnelling mechanisms [15]. A model of filamentary conduction was introducted by Dearnaley *et al.* [16], in which conduction takes place through highly conductive filaments, which bridge the insulating layer between the electrodes and are created during the forming process. It is believed that these filaments are essentially of metallic nature [7, 20] and will subsequently rupture when a sufficiently high local temperature is attained. This model can account for most of the observed effects and is applicable to different materials including insulators, semiconductors and polymer films. This basic model has been modified and extended by many workers [17–19].

In this work the forming effect of SiO_x films embedded between two metal electrodes, laterally spaced [8], is compared to the usual MIM sandwich structure which shows the same forming effect. Development of VCNR is studied and its dependence on ambient pressure is discussed. Breakdown behaviour due to the power lost is explained. The diffusion of the electrode material which may account for the forming effect is shown by electronmicroscopy.

2. Experimental work

Cu–SiO_x–Cu samples were evaporated at rates of 0.8 to 1.0 nm sec^{-1} (Cu) and 0.6 to 0.7 nm sec^{-1} (SiO_x) and were deposited on Corning 7059 glass substrates. All evaporation and electrical measurement procedures were as reported previously [7, 8]. Two types of device were employed: type A (conventional MIM sandwich structure) [7] and type B (planar geometry devices) [8]. Devices were formed by slowly increasing the voltage until the forming voltage was reached. All measurements were performed in a subsidiary vacuum system at approximately 10^{-6} torr unless in some cases the pressure varied between 10^{-6} torr and atmospheric pressure.

3. Results and discussion

3.1. Electroforming in Cu–SiO_x–Cu sandwich structures (type A)

Two extreme cases of forming phenomena appeared in all our samples. The first one is the typical forming in which the current is very low (1×10^{-6} A) and at a certain voltage (~ 3 V) the current rises rapidly indicating that the device is starting to form. This case is shown in Fig. 1a for a Cu–SiO_x (100 nm)–Cu device. When the voltage was reduced the higher current appeared (6×10^{-4} A) compared with 1×10^{-6} A. The peak current did not appear because the forming voltage was less than the peak voltage.

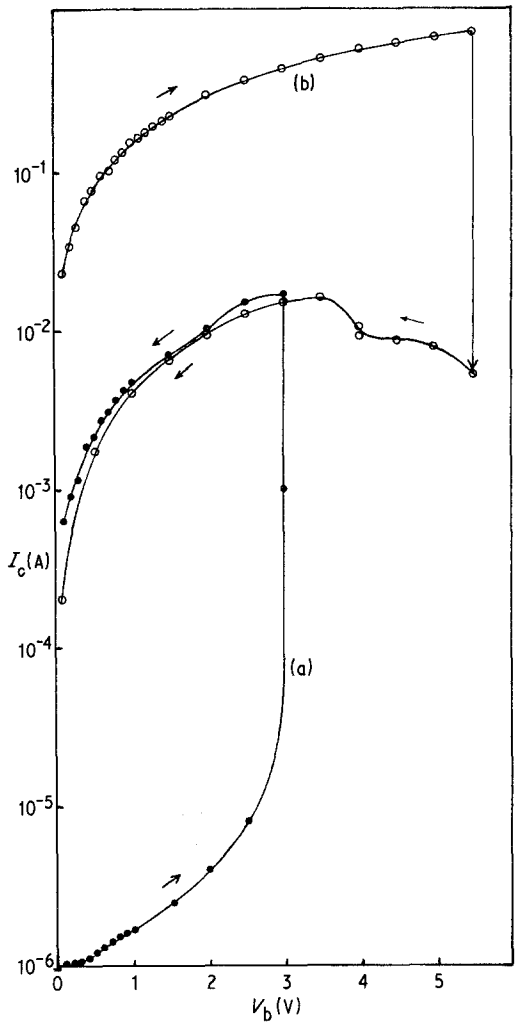

Figure 1 Electroforming of type A devices of Cu–SiO_x–Cu at room temperature. Sample thickness (a) 110 nm, (b) 86 nm.

The second case displayed higher currents before forming (~ 2×10^{-2} A), and this was quite different from the first case. The current increased with voltage until it reached a certain voltage (5.5 V) when it dropped to 5×10^{-3} A from 7.5×10^{-1} A. In reducing the voltage a negative resistance appeared with peak current at 3.5 V and the current continued to fall whilst reducing the voltage to a value 2×10^{-4} A (at 0.1 V) compared with 2×10^{-2} A. This case is shown in Fig. 1b for a

Cu–SiO_x (86 nm)–Cu device with edge thickening (280 nm).

The important point in the figures is that the conductivity of the unformed device seems to have no effect on the formed samples, where the characteristic falls into the same level of current after forming.

The high current in the second case is not uncommon in thin film devices [21, 22], and is usually taken as an indication of a short circuit between the electrodes, electrode diffusion, porosity of SiO layer or the absorption of water vapour during evaporation or subsequent transferral to the test system. Since our sample is thickened at the edges and reasonably thick, the possibility of a short circuit is weak, but the latter possibilities appear to be likely to happen as SiO becomes hygroscopic in a poor vacuum containing water vapour at lower source temperature [23]. Trapped water vapour would lead to a greatly increased current density and the high temperatures thus generated would lead to evaporation or to melting of the low resistance paths.

3.2. The forming process of thin SiO_x films with laterally spaced electrodes (type B)

In this type of device the first cycle before forming always displayed a high current up to 0.9 A, which is almost similar in form to Fig. 1b for MIM sandwich devices, but the current did not always drop to a lower value and sometimes started to saturate at a certain voltage (5 V), maintaining the same value up to ~ 30 V then dropping to zero (breakdown). The two cases are shown in Fig. 2. As we mentioned before the high current is probably due to the absorption of water vapour not only during evaporation, but also when it is transferred to the measuring system, especially the type of devices where the insulator is not sandwiched between the electrodes (open structure). Moreover, short circuits occur as predicted in the calculation of the effective separation of the electrodes [24].

Up to 4.5 or 5 V almost all these type of devices exhibit the same I_c–V_b characteristic, but after 5 V they exhibit different breakdown characteristics. As we mentioned earlier, either the current starts to saturate at 5 V up to a certain voltage where breakdown occurs, or a breakdown process starts at 4.5 to 5 V, where the current fluctuates and drops to very small levels (~ 5×10^{-2} A) compared with the level below 4.5 V as shown in Fig. 2.

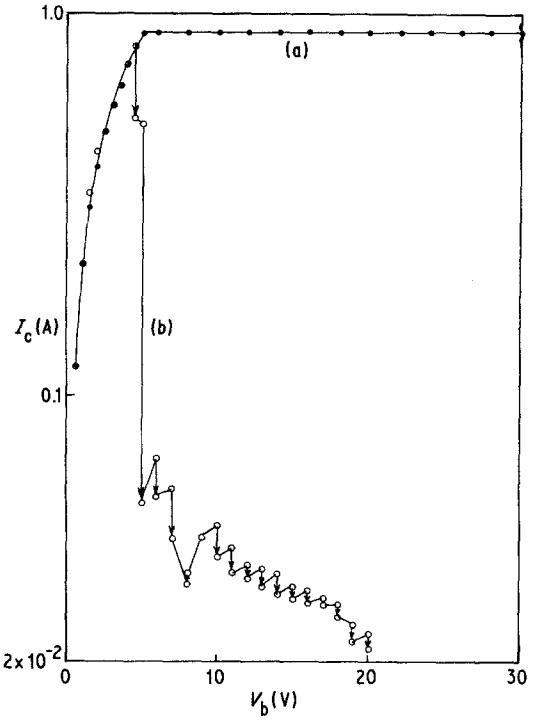

Figure 2 The first V–I cycle for two nominally identical type B devices measured at room temperature. (a) Current saturates and finally breaks down at $V_b = 30$ V. (b) Current drops at 4 V to a discontinuous lower value.

3.2.1. The power lost in the laterally spaced electrode devices (type B)

The change of power (energy lost per unit time) as a function of applied voltage is shown in Fig. 3. It can be seen that there is a reduction in the power stored in the insulator; this loss or reduction appears as heat produced in the low resistance paths between the electrodes, in the region of the insulator, by the circulating current which ultimately leads to breakdown. From Fig. 3a it can be deduced that $(dP/dV_1) = 1.5\,W\,V^{-1}$ is the slope of the curve and $(dP/dV_2) = 0.9\,W\,V^{-1}$ is the measured one. Therefore, the energy lost per unit time

$$P = \int_{V_1}^{V_2} (0.9 - 1.5)dV = -0.6[V]_{V_1}^{V_2}$$

From 0 to 5 V, $P = -3$ W, while from 5 to 30 V, $P = -15$ W. This is accompanied by an increase in the resistance from 5.25 Ω (0 to 5 V) to 26.25 Ω (5 to 30 V). In Fig. 3b, above 4.5 V almost all the power is dropped ($dP/dV \simeq 0$) and lost in breakdown processes.

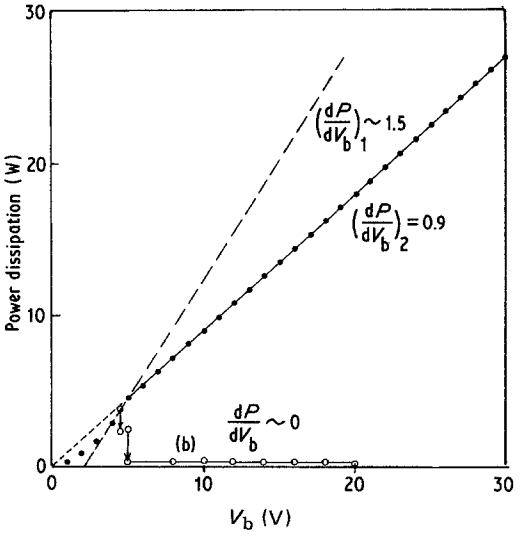

Figure 3 Power dissipation in the type B devices of Fig. 2.

3.2.2. Breakdown behaviour

Klein [25, 26] has distinguished between two types of breakdown. The first one is electronic breakdowns, which are the result of an electron avalanche inside the insulator and produce a number of holes in the material of the conventional MIM sandwich. The second one is thermal breakdowns, which occur when the power dissipation in the sample exceeds the rate at which heat can be conducted without catastrophic temperature increases. Klein designates whichever of the two processes which occurs at the lower voltage level as the maximum-voltage break-down, and the voltage at which this occurs is taken to be an intrinsic device property. In either case a self-heating breakdown occurs at voltage levels below those for maximum-voltage breakdown.

Smith and Budenstein [27] have indicated in their result that certain device areas undergo destruction at lower voltages than other areas. In NaF samples the value of the leakage current was considerably reduced after several hundred breakdowns. CaF_2 samples showed an increase in the voltage at which single-hole breakdowns take place with the number of separate breakdowns, and it was suggested that this voltage rises with the number of breakdowns due to the elimination of weak spots. Gould and Hogarth [3] noticed a discontinuous drop in the current at higher voltages, V_β, in formed SiO_x films, and refer to it as arising from burnouts to differentiate between this behaviour and the normal breakdown. In the conventional MIM sandwich

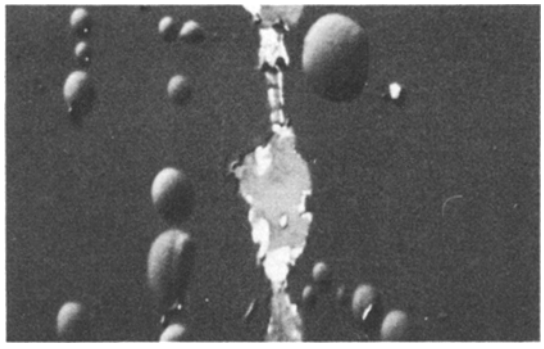

Figure 4 Electron micrograph (3 kV; × 100) of part of the inter-electrode region of a type B device.

we observed a similar breakdown to that of Gould and Hogarth [3] with $V_\beta \simeq 24$ V, but in the planar geometry devices the drop in the current is noticed at lower voltages as seen in Fig. 3b. In our device, when this happens a part of the device effective separation is peeled off due to this thermal breakdown behaviour, and also part of the electrode is peeled off due to diffusion and abnormal thermal processes. This is shown in Fig. 4.

The photograph in Fig. 4 also shows the high-field region which is assumed to exist in the insulator [3]. Destruction of layers many times the thickness of the breakdown layer have previously been reported [28]. The field at 5 V was about 1.2×10^3 V cm^{-1} which is well below the typical breakdown field at 10^6 V cm^{-1} in unformed devices [27, 28].

We believe the high field in the unformed device is created by metal atoms occupying the defect sites in the insulator and which cause a build-up of space charge, which leads to a high-field region, and which eventually discharges its current leaving part of the insulator destroyed. The current then falls abruptly to a value which is maintained by other regions of the insulator.

3.3. Development of VCNR in type B devices and the effects of ambient pressure

As mentioned earlier, from some devices the current dropped to a lower level and after that the device started to function normally. Fig. 5 shows three consecutive cycles, when the voltage in the first cycle increased to 11 V and then decreased to zero. No negative resistance appeared but the current increased in the decreasing voltage cycle, i.e. at 1 V the current increased from 1.25×10^{-4} A

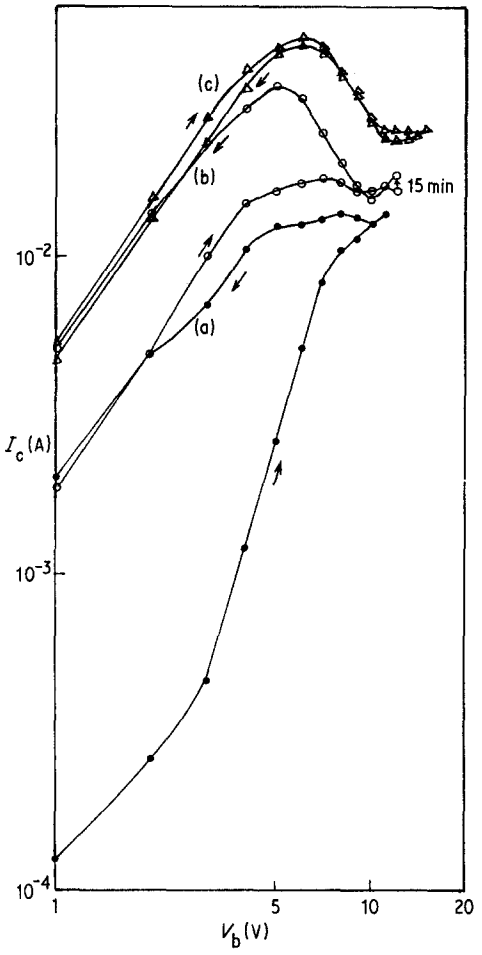

Figure 5 Development of VCNR in type B devices, (a) first cycle, (b) second cycle, (c) third cycle.

to 2×10^{-3} A. The second trace showed a small peak current at 7 V. The voltage was then increased to 12 V and left on for 15 min, when the current increased from 16 mA to 18 mA. On decreasing the voltage a higher peak current was observed at 5 V. Also the current level was higher in the decreasing cycle of voltage, i.e. at 1 V the current in the second cycle increased from 1.85 mA up to 5 mA. The third trace was more reproducible and the tracing was made up to 15 V with a peak current at 6 V. The current for increasing and decreasing voltage was almost the same. Fig. 5 shows how the conductivity and VCNR is developed in these devices.

Another identical device was electroformed in vacuum but the peak current was observed at 12 V (at 10^{-6} torr). On increasing the ambient pressure the peak current was reduced and the negative resistance region was gradually reduced

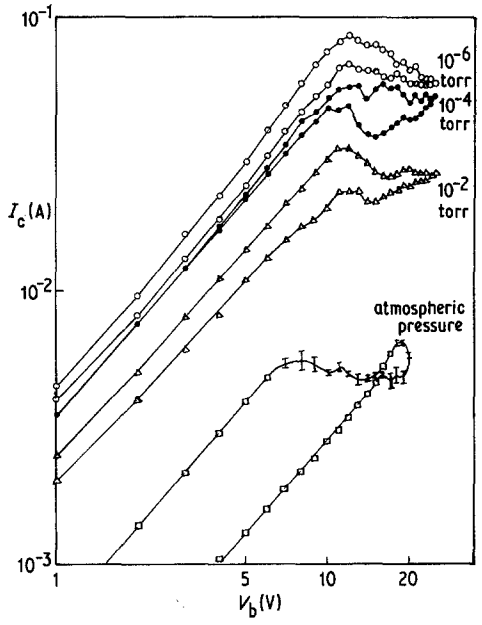

Figure 6 Effect of ambient air pressure on VCNR in type B devices.

until it disappeared just above atmospheric pressure. Below 10^{-2} torr the current is reduced on decreasing the voltage and it was significantly reduced on decreasing the voltage at atmospheric pressure. This effect is shown in Fig. 6. At atmospheric pressure, fluctuations in the current are observed above 7 V on increasing the voltage. On decreasing the voltage the current is reduced with no significant fluctuations below 15 V. This reduction in current and disappearance of VCNR at low pressure might perhaps be attributed to the oxidation of the conducting paths or to the neutralization of the traps and dangling bonds which may exist in SiO, by oxygen.

3.4. Electrode diffusion and microprobe analysis in type B devices

A knowledge of the diffusion process in thin films for applications such as in micro-electronic devices is important for the design, fabrication and reliability of the thin film package. The reliability problems in thin film devices involves diffusion driven by electron or phonon currents rather than by chemical gradients. The diffusion rates expected move along the high density of defects which exist in thin films.

Fig. 7a is an electron micrograph of a type B device prepared with a laterally spaced electrodes. The darker part shows the copper electrodes and the lighter is of silicon monoxide (the effective

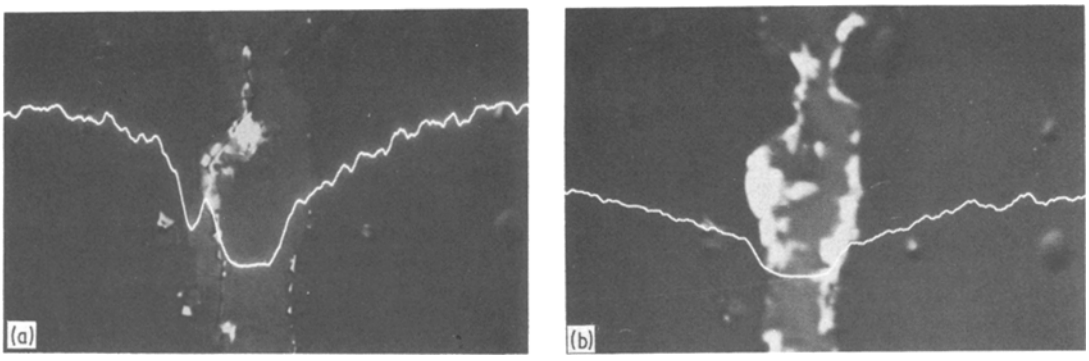

Figure 7 (a) Electron micrograph and line scan of copper for part of the inter-electrode region of a fresh Cu–SiO_x–Cu device (×200). (b) Electron micrograph and copper line scan when 50 V is applied between electrodes (×200).

separation). A copper line scan is shown in the figure. The electron beam has been scanned across the effective separation (gap) of a freshly-prepared device and the intensity variation of the X-ray line shows there to be a copper deficient region in the gap between the electrodes (silicon monoxide). Firstly, we notice a gradual decrease in the intensity when the beam scans towards the edge of the electrode (towards the gap). This arises because the insulator (silicon monoxide) covers part of the electrode during the evaporation procedure [8]. Secondly, there is no sharp change at the edges of the gap because of the shadowing of the electrode [8, 24].

Fig. 7b shows a copper line scan of the device at 50 V, and we notice that the copper concentration has increased as a result of a thermal/field-enhanced interdiffusion of filamentry paths through the oxide which accounts for the electroforming process.

The bright (white) areas in Fig. 7a arise from the peeled-off insulator, because of the absorption of vapour. These areas are increased at 50 V due to electrode interdiffusion in some parts and lead to peeling off more areas of the insulator, Fig. 7b. This interdiffusion occurred in some localized parts of the insulator, but not along the whole area, because the filament established itself through a few low resistance paths in certain areas with respect to other parts of a high resistance area in the insulator matrix. This interdiffusion might help in generating the filaments to account for the forming effect.

4. Conclusion

Two extreme cases of forming were observed in type A devices. The first case is the ordinary forming effect in which the device formed at ~ 3 V where the current increased to a higher level. The second case showed a higher current level in the first cycle before forming. This high current is believed to be partly due to short circuiting and partly due to absorption of water vapour. This high current density and high temperature thus generated could lead to evaporation or to melting of the low resistance paths. The water vapour at the same time may dissociate to hydrogen and oxygen ions. The oxygen ions may react with the silicon atoms or may be extracted from the device by the high-field region. The hydrogen ions may become mobile and contribute to the conduction which leads to such high current density. The important point is that the conduction of the unformed type A devices seems to have no correlation with the properties of the formed devices. Most of type B devices had displayed a high current density in the first new cycles, similar to that of type A devices in the second case. Most devices exhibited the same characteristic up to 5 V; beyond that the current either saturated or dropped to a lower level. This drop in the current is due to a high power loss in the device accompanied by an increase in the resistance. Electron microscopic examination showed that this would lead to the destruction of part of the effective separation where part of the electrodes is peeled off and part of it diffused into the insulator due to abnormal thermal/field enhanced processes.

The high field in the unformed devices may be created by metal atoms occupying the defect sites in the insulator which causes a build-up of space-charge which leads to a high-field region and eventually discharges its current leaving part

of the insulator destroyed. The dissociation of water vapour may count for the high current as explained earlier in type A devices. The current falls abruptly to a value which is maintained by other regions of the insulator. The field is well below the breakdown field which leads to the destruction of the whole device. The devices function normally after eliminating such high conduction states.

The forming voltage in type B devices varies from sample to sample, but generally VCNR can be produced if consecutive voltage cycling is applied. The thermal/field-enhanced interdiffusion of filamentary paths through the low resistance paths in the insulator may account for this forming effect, as confirmed by electron microscopy.

The peak current is usually observed at higher voltages than in type A devices. The peak current is reduced with increasing ambient pressure. At atmospheric pressure, fluctations in the current are observed when disappearance of the peak and pressure–memory effect is obtained. This disappearance may be attributed to oxidation of the conduction paths.

References

1. G. S. KREYNINA, L. N. SELIVANOV and T. I. SHUMSKAIA, *Radio Eng. Electron Phys.* **5** (1960) 219.
2. R. R. VERDERBER, J. G. SIMMONS and B. EALES, *Phil. Mag.* **16** (1967) 1049.
3. R. D. GOULD and C. A. HOGARTH, *Int. J. Electron.* **37** (1974) 157.
4. *Idem, ibid.* **38** (1975) 577.
5. *Idem, Phys. Status Solidi (a)* **41** (1977) 439.
6. *Idem, ibid.* **55** (1979) 325.
7. S. A. Y. AL-ISMAIL and C. A. HOGARTH, *ibid.* **76** (1983) 559.
8. *Idem, J. Mater. Sci.* **18** (1983) 2777.
9. J. G. SIMMONS and R. R. VERDERBER, *Proc. R. Soc.* **A301** (1967) 77.
10. A. K. JONSCHER, *Thin Solid Films* **1** (1967) 213.
11. R. BLESSING and H. PAGNIA, *ibid.* **52** (1978) 333.
12. G. DEARNALEY, A. M. STONEHAM and D. V. MORGAN, *Rep. Prog. Phys.* **33** (1970) 1129.
13. T. W. HICKMOTT, *J. Appl. Phys.* **35** (1964) 2679.
14. P. D. GREENE, E. L. BUSH and I. R. RAWLINGS, "Proceedings of the Symposium on Deposited Thin Film Dielectric Materials", edited by F. Vranty (The Electrical Society, New York, 1968) p. 167.
15. C. BARRIAC, P. PINARD and F. DAVOINE, *Phys. Status Solidi* **34** (1969) 621.
16. G. DERNALEY, D. V. MORGAN and A. M. STONEHAM, *J. Non-Cryst. Solids* **4** (1970) 593.
17. R. R. SUTHERLAND, *J. Phys.* **D4** (1971) 468.
18. J. E. RALPH and J. M. WOODCOCK, *J. Non-Cryst. Solids* **7** (1972) 236.
19. A. E. RAKHSHANI, C. A. HOGARTH and A. A. ABIDI, *ibid.* **20** (1976) 25.
20. C. A. HOGARTH and M. NADEEM, *Phys. Status Solidi (a)* **56** (1979) K37.
21. R. R. SUTHERLAND, J. P. WILLIAMSON and R. A. COLLINS, *J. Phys. D: Appl. Phys.* **5** (1972) 1686.
22. R. D. GOULD and C. A. HOGARTH, *Phys. Status Solidi (a)* **23** (1974) 531.
23. N. SCHWARTZ and R. W. BERRY, "Physics of Thin Films", Vol. 2, edited by G. Hass and R. E. Thun (Academic Press, New York, 1964) p. 401
24. S. A. Y. AL-ISMAIL, PhD thesis, Brunel University (1982).
25. N. KLEIN, *J. Electrochem. Soc.* **116** (1969) 983.
26. *Idem, Thin Solid Films* **7** (1971) 149.
27. J. L. SMITH and P. P. BUDENSTEIN, *J. Appl. Phys.* **40** (1969) 3491.
28. P. P. BUDENSTEIN, P. J. HAYES, J. L. SMITH and W. B. SMITH, *J. Vac. Sci. Technol* **6** (1969) 289.

Received 18 July
and accepted 31 July 1984